

# Online Research @ Cardiff

This is an Open Access document downloaded from ORCA, Cardiff University's institutional repository: <https://orca.cardiff.ac.uk/id/eprint/126025/>

This is the author's version of a work that was submitted to / accepted for publication.

Citation for final published version:

Abis, Laura, Dimitratos, Nikolaos ORCID: <https://orcid.org/0000-0002-6620-4335>, Meenakshisundaram, Sankar ORCID: <https://orcid.org/0000-0002-7105-0203>, Freakley, Simon J. and Hutchings, Graham J. ORCID: <https://orcid.org/0000-0001-8885-1560> 2019. Plasmonic oxidation of glycerol using AuPd/TiO<sub>2</sub> catalysts. *Catalysis Science and Technology* 9 (20) , pp. 5686-5691. 10.1039/C9CY01409H file

Publishers page: <http://dx.doi.org/10.1039/C9CY01409H>  
<<http://dx.doi.org/10.1039/C9CY01409H>>

Please note:

Changes made as a result of publishing processes such as copy-editing, formatting and page numbers may not be reflected in this version. For the definitive version of this publication, please refer to the published source. You are advised to consult the publisher's version if you wish to cite this paper.

This version is being made available in accordance with publisher policies.

See

<http://orca.cf.ac.uk/policies.html> for usage policies. Copyright and moral rights for publications made available in ORCA are retained by the copyright holders.



# **Plasmonic oxidation of glycerol using AuPd/TiO<sub>2</sub> catalysts**

Laura Abis,<sup>1</sup> Nikolaos Dimitritatos,<sup>1</sup> Meenakshisundaram Sankar,<sup>1</sup> Simon J. Freakley<sup>1,2</sup> and Graham J. Hutchings<sup>1\*</sup>

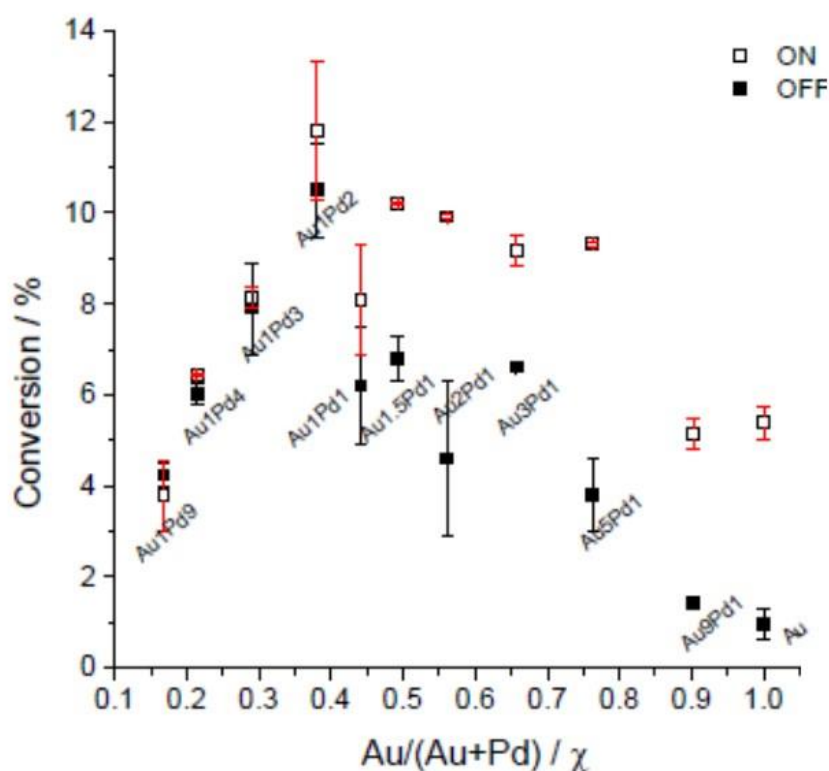
<sup>1</sup> Cardiff Catalysis Institute, School of Chemistry, Cardiff University, Main Building, Park Place, Cardiff, CF10 3AT, UK.

<sup>2</sup> Department of Chemistry, University of Bath, Claverton Down, Bath, BA2 7AY, UK

## Abstract

AuPd nanoparticles supported on P25 TiO<sub>2</sub> (AuPd/TiO<sub>2</sub>) were prepared by a facile sol-immobilisation method and investigated for surface plasmon-assisted glycerol oxidation under base-free conditions. The AuPd/TiO<sub>2</sub> samples were characterized by UV-vis spectroscopy and transmission electron microscopy. The sol-immobilisation method readily permitted the Au:Pd molar ratio to be changed over a wide range whilst keeping the mean particle size of the AuPd nanoparticles at 3nm. Visible light irradiation during the reaction has a beneficial effect on the conversion of glycerol with the most marked effect being observed with gold-rich catalysts and the increase of conversion on light irradiation increases linearly with the gold content of the nanoparticles. The reaction selectivity is also affected by the plasmon-assisted oxidation and glycolic acid, not observed during the dark reactions, was observed for all illuminated reactions due to the enhanced activity of these catalysts.

## Graphical Abstract



## Introduction

Glycerol is a by-product of biodiesel manufacturing and is a highly functionalised molecule which could be a viable starting material for the production of many important derivatives in the fine chemicals industry.<sup>1-3</sup> The selective oxidation of glycerol has been extensively studied as a means of converting glycerol to potentially valuable products such as glyceric acid, tartronic acid and dihydroxyacetone.<sup>4,5</sup> Supported Au catalysts have been shown to be highly active for glycerol oxidation to glyceric acid at high pH.<sup>6,7</sup> The high pH is required to activate the hydroxyl group of glycerol by H-abstraction and catalysts that are active at high pH are not necessarily active at neutral pH. Addition of Pd to Au can enhance the activity but in general basic conditions are required to observe activity with gold-containing catalysts. Indeed, although there are reports of base-free oxidation of glycerol with Au catalysts these tended to utilise basic supports such as MgO and these are found to dissolve during the reaction in sufficient amounts to induce the basic environment required for selective oxidation.<sup>8</sup> Hence new approaches are required to observe catalysed base-free oxidation of glycerol, preferred from a green chemistry and cost-saving perspective.

Plasmonic photocatalysis is an emerging field which aims to utilise renewable energy to power chemical reactions. This approach exploits the plasmonic properties of noble metal nanoparticles, in particular those containing Au, to harvest visible light due to the localized surface plasmon resonance effect (LSPR) and this can then be transferred as a potential method to convert renewable energy into chemical energy.<sup>9-17</sup> Several studies have been conducted for selective alcohol oxidation driven by plasmonic photocatalysis.<sup>18-26</sup> To date glycerol oxidation has been studied in limited detail using traditional photocatalysts based on Au.<sup>27-33</sup> Recent studies have shown that base-free glycerol oxidation can be accelerated using catalysts capable of LSPR under visible light illumination. These earlier studies have used monometallic Au catalysts that contain significant amounts of gold, typically > 5% wt to see pronounced effects. In many studies of thermally-induced glycerol oxidation, a synergy between Au and Pd is commonly seen and results in an enhancement in activity.<sup>8</sup> In this study we show that AuPd alloys supported on TiO<sub>2</sub> prepared using sol-immobilisation can be very effective for the plasmonic photocatalysis of glycerol and that these catalysts are active using only 1 % wt of the noble metal.

## Experimental

### Preparation of 1% wt AuPd/TiO<sub>2</sub> catalysts

Bimetallic (1% wt AuPd/TiO<sub>2</sub> (molar ratio Au:Pd 1:1)) catalysts were prepared by sol-immobilisation using polyvinyl alcohol (PVA) as a stabilising polymer. In a typical catalyst synthesis (1 g), an aqueous solution of HAuCl<sub>4</sub>·3H<sub>2</sub>O (0.8 mL, 12.5 mg Au/mL Sigma Aldrich, metal content ≥49.0%) and PdCl<sub>2</sub> (Sigma Aldrich, Reagent Plus<sup>®</sup> 99%, 6 mg Pd/mL) were added to 400 mL of deionised water with stirring, followed by the addition of a polymer stabilizer (PVA 1 % wt aqueous solution (average molecular weight  $M_w = 9000-10000$  g/mol, 80% hydrolysed), polymer/metal = 0.65 by weight). Subsequently, a freshly prepared solution of NaBH<sub>4</sub> (≥99.99%, Aldrich, 0.1 M) was added (mol NaBH<sub>4</sub>/mol Au = 5) to form a red sol. After 30 min, the colloid was immobilised by adding 0.99 g of TiO<sub>2</sub> (P25 Aeroxide<sup>®</sup>, Evonik) together with concentrated H<sub>2</sub>SO<sub>4</sub> (1 ml). After 1 h of continuous stirring, the slurry was filtered, and the catalyst was recovered by filtration and washed thoroughly with deionised water and dried (110 °C, 16 h). A series of 1% wt AuPd/TiO<sub>2</sub> catalysts with different Au:Pd molar ratios using the same procedure but with the different relative amounts of Au and Pd.

### Glycerol Oxidation

Plasmonic oxidation of glycerol was carried out using a reactor design based on previously reported setups<sup>33</sup>, and comprised a stainless steel custom designed autoclave reactor built by DG Innovation. The reactor consisted of a borosilicate window, gas inlet, outlet, thermocouple inlet, pressure gauge and pressure release valve, and a vessel where the reaction liner was located. A glass vial (15 mL) was placed in a Teflon jacket (2.5 cm diameter) and wrapped in aluminium foil to ensure thermal contact, The maximum operating pressure of the reactor, determined by the presence of the window, is 11 bar. The maximum operating volume is 7.5 mL. Heating was provided by a heating mantle designed, connected to a control box (K39 Ascon Tecnologic, assembled by Elmatic, Cardiff). The light source is a 300 W lamp (USHIO) (ORIEL OPL-500). For all experiments IR radiation was removed from the output light by a water filter, and wavelengths below 420 nm were eliminated through a cut-off filter (Newport Stablif<sup>®</sup> Technology). The filtered light was focused on the top of the reactor through a 90° mirror.

Plasmonic photocatalytic glycerol oxidation at pH 7 was carried out under dark and illuminated conditions with aqueous glycerol (5 ml, 0.05 M), catalyst (5 mg), Gly/Au = 130. After addition of the reactants the reactor was sealed, flushed with 5 bar O<sub>2</sub> five times and finally pressurised

with O<sub>2</sub> (continuously supplied). The temperature was set to 90 °C and the experiment started when temperature in the heating mantle reached the selected value. Total reaction time was 3 h. After reaction, the reactor was rapidly quenched in an ice bath, the liner weighed and the slurry collected, filtered through a micropore PTFE filter (0.25 μm) and directly injected to HPLC for analysis. Product analysis was carried out using an Agilent 1260 Infinity HPLC with a Metacarb 67H column with a 0.1 % wt solution of phosphoric acid as mobile phase.

### **Catalyst characterisation**

The plasmon resonance characteristics of the AuPd catalysts was determined using UV-visible spectroscopy. The metal content of the catalysts was determined Inductively Coupled Plasma – Mass Spectrometry (Agilent 7900 ICP-MS) following digestion of the catalyst in aqua regia. Transmission electron microscopy analysis was performed using a JEOL 2100 microscope with a LaB<sub>6</sub> filament operating at 200 kV. Samples were prepared by dispersing the catalyst in ethanol and allowing a drop of suspension to evaporate on a lacey carbon film supported over a 300 mesh copper TEM grid.

### **Results and Discussion**

A series of bimetallic 1% wt AuPd/TiO<sub>2</sub> with different Au:Pd molar ratios were prepared by sol-immobilisation using PVA as stabilising agent. Table 1 shows the catalyst series with the corresponding nominal molar fractions and experimentally metal ratio determined by ICP analysis allowing the variation of activity with metal composition to be determined. Gold exhibits a strong surface plasmon resonance in the visible region<sup>34</sup> whereas palladium exhibits a strong surface plasmon resonance in the 200-400 nm spectral region.<sup>35</sup> Previous studies have shown that the presence of Pd in the surface of Au nanoparticles suppresses the gold plasmon resonance in the visible region,<sup>36,37</sup> as shown in Figure 1. TiO<sub>2</sub> does not have any absorption in the visible region<sup>37</sup> and; in addition, as we use a cut off filter of 420 nm no UV is going into the reactor so the TiO spectrum is not shown in Figure 1. Of all the samples, only the Au<sub>9</sub>Pd<sub>1</sub> catalyst showed a clear plasmonic peak at about 550 nm, as expected from its higher gold loading and this decreased significantly with higher Pd loadings. Transmission electron microscopy of the catalysts, Figure 2, did not show any particle size dependence of the Au/Pd ratio. The nanoparticles appear to be generally spherical and well dispersed on the support which is consistent with our previous observations for this preparation method<sup>38</sup>. The size distribution derived from counting 100 nanoparticles showed similar mean particle size 2.6 -

3.3 nm with similar standard deviations, suggesting that the metal ratio is not influencing the morphology of the nanoparticles as can be expected with the colloidal synthesis of these bimetallic metal nanoparticles.

**Table 1** 1% wt AuPd/TiO<sub>2</sub> catalysts prepared *via* sol-immobilisation method

Catalyst	Theoretical Au/(Au+Pd)	Experimental Au/(Au+Pd)	
Au<Pd	Au <sub>1</sub> Pd <sub>9</sub>	0.10	0.17
	Au <sub>1</sub> Pd <sub>4</sub>	0.20	0.21
	Au <sub>1</sub> Pd <sub>3</sub>	0.25	0.29
	Au <sub>1</sub> Pd <sub>2</sub>	0.33	0.38
	Au <sub>1</sub> Pd <sub>1</sub>	0.50	0.44
Au>Pd	Au <sub>1.5</sub> Pd <sub>1</sub>	0.60	0.49
	Au <sub>2</sub> Pd <sub>1</sub>	0.67	0.56
	Au <sub>3</sub> Pd <sub>1</sub>	0.75	0.66
	Au <sub>5</sub> Pd <sub>1</sub>	0.83	0.76
	Au <sub>9</sub> Pd <sub>1</sub>	0.90	0.90

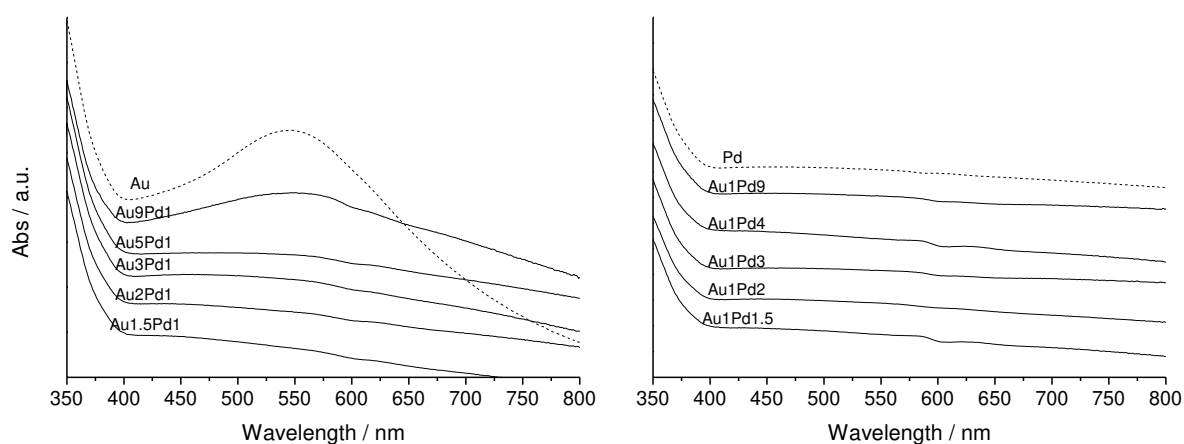


**Figure 1** Diffuse Reflectance UV-Vis of 1% wt AuPd/TiO<sub>2</sub> catalysts Au rich and Pd rich, compared with the spectra of pure 1% wt Au/TiO<sub>2</sub> and 1% wt Pd/TiO<sub>2</sub>.

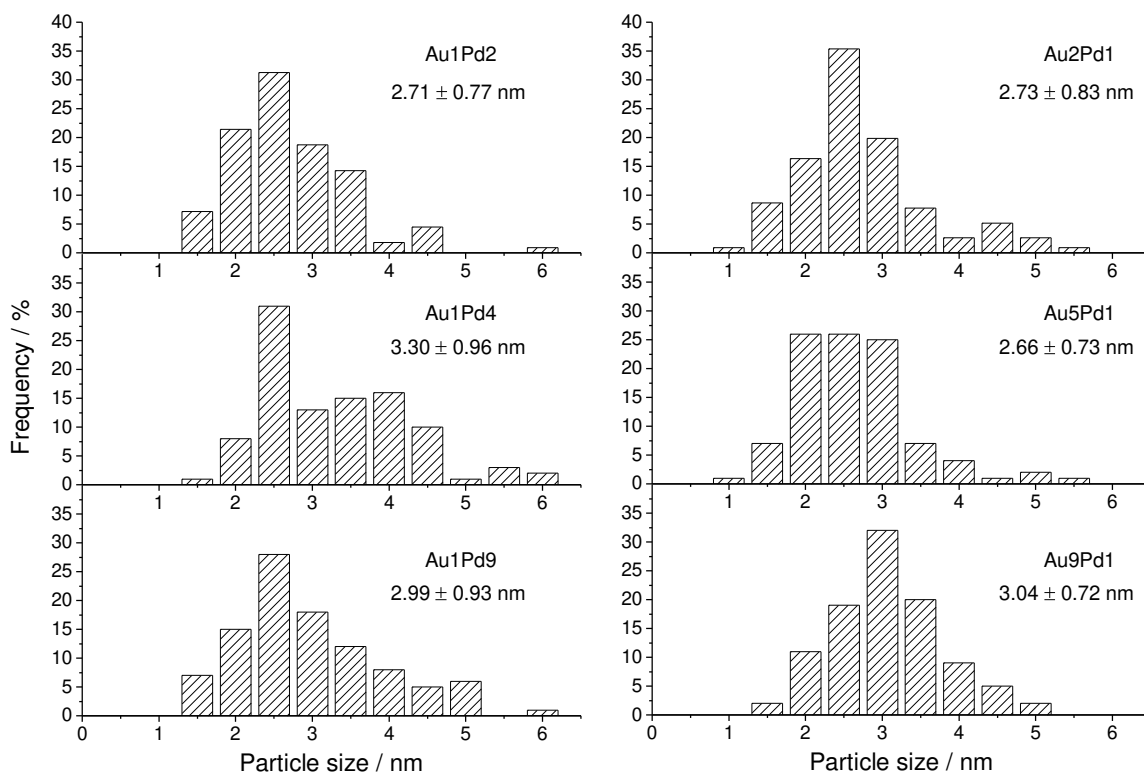


**Figure 2** –Particle size distribution determined by TEM for a representative selection of 1% wt AuPd/ TiO<sub>2</sub> selected catalysts

Figure 3 shows glycerol conversion under illumination and dark conditions *versus* the gold molar fraction for the 1% wt AuPd/TiO<sub>2</sub> series. As has been observed in previous studies of AuPd alloy catalysts for alcohol oxidation there is a pronounced synergy and maximum in conversion for the bimetallic alloy catalysts.<sup>8</sup> In principle, it is possible to observe two different trends for the catalysts, depending on the gold and palladium content centered around the Au:Pd = 1 catalyst. The Pd-rich catalysts, as expected,<sup>39</sup> are more active under dark conditions but they do not show a marked enhancement in activity when illuminated. Conversely, the gold-rich catalysts were less active under dark conditions, but when illuminated they showed a higher conversion enhancement and the enhancement in conversion increased with increasing gold content.



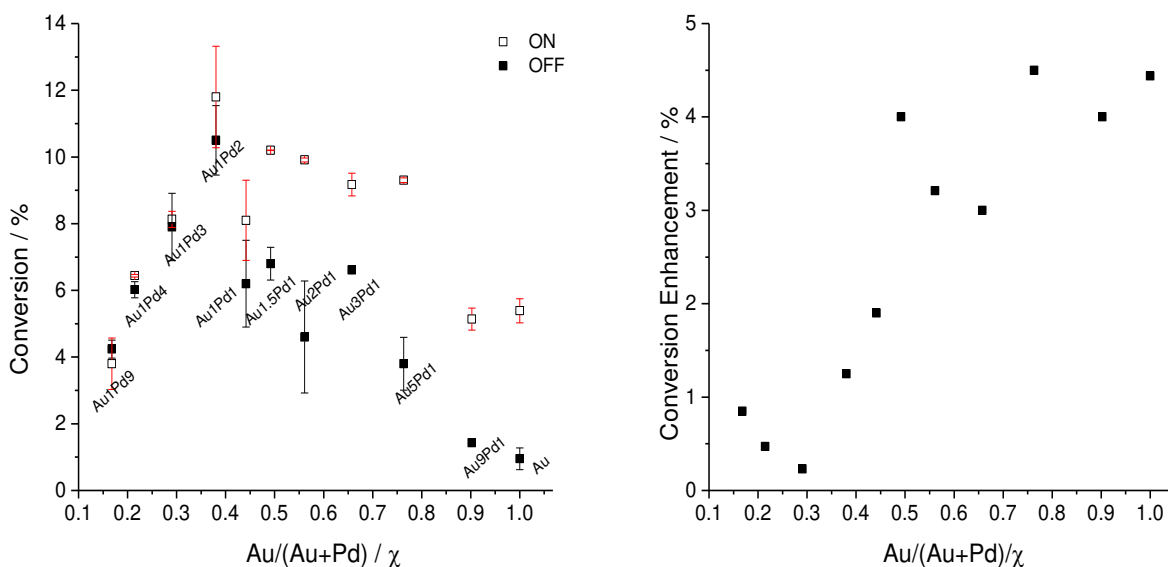


**Figure 3** Catalytic performance of AuPd/TiO<sub>2</sub> catalysts for glycerol oxidation under dark and illumination conditions

Figure 4 shows the selectivity to the major products of glycerol oxidation under dark and illuminated reaction conditions. The lower carbon mass balance observed for the illuminated samples has been suggested to be linked to a higher H<sub>2</sub>O<sub>2</sub> production under these conditions,<sup>40,41</sup> which favours the over-oxidation of products to CO<sub>2</sub>. The production of H<sub>2</sub>O<sub>2</sub> on Au nanoparticles has been documented also in dark conditions.<sup>42-44</sup> In particular, in their studies on CO oxidation and glycerol oxidation in basic conditions, Davis and co-workers<sup>42,43</sup> demonstrated, with the support of DFT calculations, that O<sub>2</sub> acts as a scavenger of the electrons accumulated on the Au nanoparticle after the substrate oxidation, thereby closing the catalytic cycle. They proposed that the H<sub>2</sub>O<sub>2</sub> detected in the solution arises from the reduction of O<sub>2</sub> on Au surface, in a process that eventually leads to the regeneration of the hydroxide ions. The H<sub>2</sub>O<sub>2</sub> formed reacts with the products of glycerol oxidation leading to carbon-carbon bond scission resulting in products with lower carbon number and eventually CO<sub>2</sub>. Since AuPd nanoparticles have been previously shown to be more active than Au for the synthesis of H<sub>2</sub>O<sub>2</sub><sup>45</sup> this effect can be expected to be enhanced. Low amounts of tartronic acid and glyceraldehyde were detected for all the catalysts at similarly low levels for all catalysts but due to the high levels of uncertainty at low concentration are omitted from figure 4.

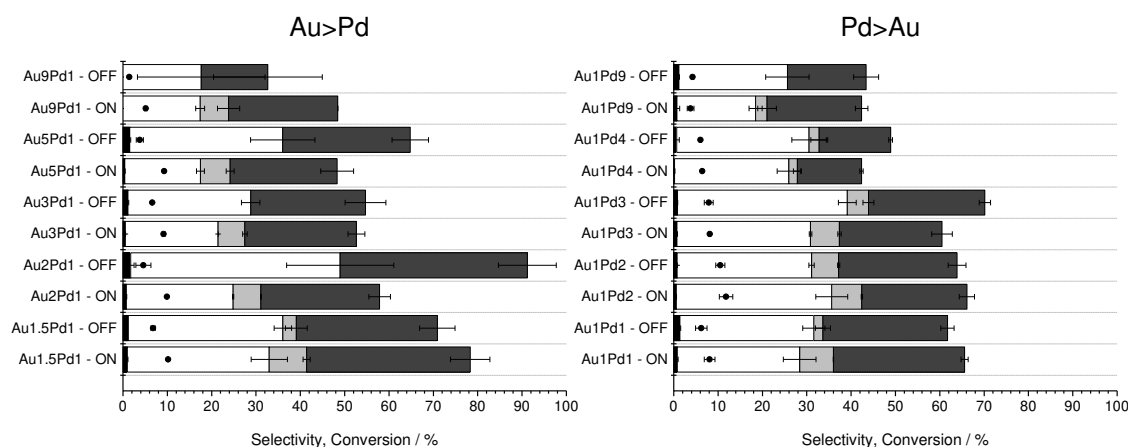


**Figure 4** Conversion and selectivity to the principle reaction products for the AuPd catalysts under dark and illumination conditions. *Reaction conditions:* 5 mL glycerol 0.05 M, 5 mg catalyst, 90 °C, 3 h. *Key:* ● (black dot) glycerol conversion; ■ (light grey) pyruvic acid (PA); □ (white) glyceric acid (GA); ■ (dark grey) glycolic acid (GLYA); ■ (black) dihydroxyacetone (DHA); remaining product is CO<sub>2</sub>. For reference: Au only catalyst; light off 1.2% conversion, 56% GA, 44% DHA; light on 5% conversion, 9% GA, 16% GLYA, 22% DHA.

Taking into consideration the experimental errors, which are greater at lower conversions, a general trend can be observed that there is a higher selectivity to C<sub>3</sub> products under dark conditions. At higher Au content (Au>1.5, Figure 4) under dark conditions, the formation of glycolic acid is not favoured. Conversely, when the Pd-rich catalysts were used, glycolic acid was present under both conditions for all the catalysts excluding the Au<sub>1</sub>Pd<sub>9</sub> and the Au<sub>1</sub>Pd<sub>1.5</sub>. The formation of glycolic acid is the result of carbon-carbon bond scission due to the higher activity of the Pd-containing catalysts. The formation of glycolic acid (a C<sub>2</sub> product) leads to the formation of CO<sub>2</sub> as a byproduct. This may be related to a different reaction mechanism under illumination conditions, due to enhanced H<sub>2</sub>O<sub>2</sub> production. Sarina *et al.*<sup>25,46</sup> studied the performance of bimetallic 3% wt AuPd catalysts supported on ZrO<sub>2</sub> for a wide series of plasmonic enhanced reactions including Suzuki-Miyaura coupling, benzyl alcohol oxidation, and the dehydrogenation of alcohols. They proposed that the origin of the activity of the bimetallic catalysts is related to the electronic heterogeneity of the alloy, whereby the electrons can flow across the Au and Pd interface to equalise the chemical potential throughout the alloy nanoparticle.<sup>25</sup> Since the nanoparticles are able to absorb in the visible region, when

illuminated, the additional energised electrons are also transported, enhancing the catalytic activity.<sup>25,46</sup> In our study we confirm the enhanced activity for AuPd alloys under visible light illumination and also show that the selectivity can be influenced by excitation of the plasmon resonance. In addition, we show this effect with much lower metal loadings as previous studies have used much higher metal contents ( $\geq 3$  % wt) and we show for the first time that by using the sol-immobilisation preparation method much lower metal contents can be used to demonstrate the effects.

## Conclusions

It was shown that visible light irradiation triggered the plasmonic properties of AuPd alloy nanoparticles and that in the presence of visible light illumination higher activities of base-free glycerol oxidation can be observed. The addition of Pd induces a synergistic effect with the highest activity being observed with the Au:Pd 1:2 molar ratio AuPd/TiO<sub>2</sub> alloy catalyst. However, the enhanced conversion observed on illumination is most pronounced with gold rich catalysts, which can be expected from the intensity of the plasmon resonance. Plasmon driven reactions produce higher amounts of H<sub>2</sub>O<sub>2</sub> which is a typical intermediate in photocatalytic reactions, and this leads to C–C cleavage and produces glycolic acid. This study has shown that the effects of using the plasmon resonance can be readily observed with low amounts of the noble metal opening up further possibilities for catalyst design.

## Acknowledgements

This work is supported by Cardiff University and the MAXNET Energy research consortium of the Max Planck Society and we thank Georgios Dodekatos and Harun Tüysüz for their advice and assistance with the reactor design.

## References

1. M. Pagliaro, R. Ciriminna, H. Kimura, M. Rossi and C. Della Pina, *Angew. Chem. Int. Ed.*, 2007, **46**, 4434-4440.
2. C. H. Zhou, J. N. Beltramini, Y. X. Fan and G. Q. Lu, *Chem. Soc. Rev.*, 2008, **37**, 527-549.

3. A. Behr, J. Eilting, K. Irawadi, J. Leschinski and F. Lindner, *Green Chem.*, 2008, **10**, 13-30.
4. B. Katryniok, H. Kimura, E. Skrzynska, J. S. Girardon, P. Fongarland, M. Capron, R. Ducoulombier, N. Mimura, S. Paul, F. Dumeignil, *Green Chem.*, 2011, **13**, 1960-1979.
5. A. Villa, N. Dimitratos, C. E. Chan-Thaw, C. Hammond, L. Prati and G. J. Hutchings, *Acc. Chem. Res.*, 2015, **48**, 1403-1412.
6. S. Carretin, P. McMorn, P. Johnston, K. Griffin and G.J. Hutchings, *Chem. Commun.*, 2002, 696-697.
7. C.D Evans, S.A. Kondrat, P.J. Smith, T.D Manning, P.J. Miedziak, G.L. Brett, R.D. Armstrong, J.K. Bartley, S.H. Taylor, M.J. Rosseinsky and G.J. Hutchings, *Faraday Discussions*, 2016, 188, 427-450
- 8 J.L. Fu, Q. He, P.J. Miedziak, G.L. Brett, X.Y. Huang, S. Pattission, M. Douthwaite and G.J. Hutchings *Chem. Eur. J.*, 2018, **24**, 2396-2402
9. K. Awazu, M. Fujimaki, C. Rockstuhl, J. Tominaga, H. Murakami, Y. Ohki, N. Yoshida and T. Watanabe, *J. Am. Chem. Soc.*, 2008, **130**, 1676–1680.
10. P. Christopher, D. B. Ingram and S. Linic, *J. Phys. Chem. C*, 2010, **114**, 9173–9177.
11. D. B. Ingram, P. Christopher, J. L. Bauer and S. Linic, *ACS Catal.*, 2011, **1**, 1441–1447.
12. P. Christopher, H. L. Xin, A. Marimuthu and S. Linic, *Nat. Mater.*, 2012, **11**, 1044–1050.
13. X. Zhou, G. Liu, J. Yu and W. Fan, *J. Mater. Chem.*, 2012, **22**, 21337–21354.
14. P. Wang, B. B. Huang, Y. Dai and M. H. Whangbo, *Phys. Chem. Chem. Phys.*, 2012, **14**, 9813–9825.
15. M. J. Kale, T. Avanesian and P. Christopher, *ACS Catal.*, 2014, **4**, 116–128.
16. M. R. Khan, T. W. Chuan, A. Yousuf, M. N. K. Chowdhury and C. K. Cheng, *Catal. Sci. Technol.*, 2015, **5**, 2522–2531.
17. G. Dodekatos, S. Schünemann and H. Tüysüz, *Top. Curr. Chem.*, 2016, **371**, 215–252.
18. Y. Shiraishi and T. Hirai, *J. Photochem. Photobiol., C*, 2008, **9**, 157–170.
19. W. Y. Zhai, S. J. Xue, A. W. Zhu, Y. P. Luo and Y. Tian, *ChemCatChem*, 2011, **3**, 127–130.

20. A. Tanaka, K. Hashimoto and H. Kominami, *Chem. Commun.*, 2011, **47**, 10446–10448.
21. A. Tanaka, K. Hashimoto and H. Kominami, *J. Am. Chem. Soc.*, 2012, **134**, 14526–14533.
22. D. Tsukamoto, Y. Shiraishi, Y. Sugano, S. Ichikawa, S. Tanaka and T. Hirai, *J. Am. Chem. Soc.*, 2012, **134**, 6309–6315.
23. X. G. Zhang, X. B. Ke and H. Y. Zhu, *Chem. – Eur. J.*, 2012, **18**, 8048–8056.
24. Y. Sugano, Y. Shiraishi, D. Tsukamoto, S. Ichikawa, S. Tanaka and T. Hirai, *Angew. Chem., Int. Ed.*, 2013, **52**, 5295–5299.
25. S. Sarina, H. Zhu, E. Jaatinen, Q. Xiao, H. Liu, J. Jia, C. Chen and J. Zhao, *J. Am. Chem. Soc.*, 2013, **135**, 5793–5801.
26. J. C. Colmenares, P. Lisowski, D. Lomot, O. Chernyayeva and D. Lisovytskiy, *ChemSusChem*, 2015, **8**, 1676–1685.
27. 68 V. Augugliaro, H. A. H. El Nazer, V. Loddo, A. Mele, G. Palmisano, L. Palmisano and S. Yurdakal, *Catal. Today*, 2010, **151**, 21–28.
28. C. Minero, A. Bedini and V. Maurino, *Appl. Catal., B*, 2012, **128**, 135–143.
29. Y. Zhang, N. Zhang, Z.-R. Tang and Y.-J. Xu, *Chem. Sci.*, 2013, **4**, 1820–1824.
30. A. Molinari, A. Maldotti, A. Bratovcic and G. Magnacca, *Catal. Today*, 2013, **206**, 46–52.
31. N. A. Hermes, A. Corsetti and M. A. Lansarin, *Chem. Lett.*, 2014, **43**, 143–145.
32. S. Schünemann, G. Dodekatos and H. Tüysüz, *Chem. Mater.*, 2015, **27**, 7743–7750.
33. G. Dodekatos and H. Tüysüz, *Catal. Sci. Technol.*, 2016, **6**, 7307–7315.
34. V. , R. Pilot, M. Frasconi, O.M. Marago and M.A. Iati, *J. Phys.:Condens. Matter*, 2017, **29**, 203002.
35. Y. Xiong, J. Chen, B. Wiley, Y. Xia, Y. Yin and Z-Y Li, *Nano Lett.*, 2005, **5**, 1237–1242.
36. M.-L. Wu, D.-H. Chen and T.-C. Huang, *Langmuir*, 2001, **17**, 3877–3883.
37. T. Jiang, C. Jia, L. Zhang, S. He, Y. Sang, H. Li, Y. Li, X Xu and H. Liu, *Nanoscale*, 2015, **7**, 209–217.
38. G.J. Hutchings and C.J. Kiely, *Acc. Chem. Res.*, 2013,**46**, 1759–1772
39. N. Dimitratos, J. A. Lopez-Sanchez, J. M. Anthonykutty, G. Brett, A. F. Carley, R. C. Tiruvalam, A. A. Herzing, C. J. Kiely, D. W. Knight and G. J. Hutchings, *Phys. Chem. Chem. Phys.*, 2009, **11**, 4952–4961.
40. M. Hoffmann and W. Bahnemann, *Chem. Rev.*, 1995, **95**, 69–96.

41. J. Schneider, M. Matsuoka, M. Takeuchi, J. Zhang, Y. Horiuchi, M. Anpo and D. W. Bahnemann, *Chem. Rev.*, 2014, **114**, 9919-9986.
42. B. N. Zope, D. D. Hibbitts, M. Neurock and R. J. Davis, *Science*, 2010, **330**, 74-78.
43. W. Ketchie, Y. Fang, M. Wong, M. Murayama and R. Davis, *J. Catal.*, 2007, **250**, 94-101.
44. W. C. Ketchie, M. Murayama and R. J. Davis, *Topics in Catalysis*, 2007, **44**, 307-317.
45. J. Edwards, B. Solsona, P. Landon, A. Carley, A. Herzing, C. Kiely and G. Hutchings, *J. Catal.*, 2005, **236**, 69-79.
46. S. Sarina, S. Bai, Y. Huang, C. Chen, J. Jia, E. Jaatinen, G. A. Ayoko, Z. Bao and H. Zhu, *Green Chem.*, 2014, **16**, 331-341.